Title

Spatial Decoding of Immune Cell Contribution to Fibroblastic Foci in Idiopathic Pulmonary Fibrosis.

Journal

American Journal of Respiratory and Critical Care Medicine, 208(6)

ISSN

1073-449X

Authors

Yang, David C

Hsu, Ssu-Wei

Li, Ji-Min

et al.

Publication Date

2023-09-15

DOI

10.1164/rccm.202303-0372le

Peer reviewed

Spatial Decoding of Immune Cell Contribution to Fibroblastic Foci in Idiopathic Pulmonary Fibrosis

David C. Yang[1]*, Ssu-Wei Hsu[1,2]*, Ji-Min Li[1,2], Justin Oldham[3], and Ching-Hsien Chen[1,2]

[1]Division of Pulmonary, Critical Care, and Sleep Medicine and [2]Division of Nephrology, Department of Internal Medicine, University of California, Davis, Davis, California; and [3]Division of Pulmonary and Critical Care Medicine, Department of Internal Medicine, University of Michigan, Ann Arbor, Michigan

ORCID IDs: 0000-0003-2657-745X (D.C.Y.); 0000-0002-6829-2412 (S.-W.H.); 0000-0003-4957-8869 (J.O.); 0000-0002-4211-9988 (C.-H.C.).

To the Editor:

Idiopathic pulmonary fibrosis (IPF) is characterized by heterogeneity, manifested as patchy lesions evident in histopathologic and radiologic findings of the lung (1). Although current technologies, such as single-cell sequencing and mass cytometry, reveal insights into various cell populations in fibrotic lungs (2), they do not provide adequate information on the spatial distribution of cell phenotypes or how gene expression within lesions is modulated by interactions between different cell populations. Immune cells, in particular, have been recognized for their role in initiating and sustaining fibrotic processes (3), but immunosuppressive approaches have shown limited benefit or even harm (1, 3), suggesting a more nuanced role of the immune system in fibrosis. Despite this, few studies to date have explored the spatial contribution of immune cells to gene expression in lung fibroblasts within fibrotic lesions (4). To address this issue, we used digital spatial profiling, a novel sequencing technology, to obtain spatial information on the interactions and modulation of fibrotic lesions by immune cells.

Methods and Results

To investigate the role of immune cells in mediating fibrosis, we utilized biopsy samples obtained from patients with IPF. We used a combination of histological staining and multiplex immunofluorescence to identify fibrotic lesions in each sample. We selected lesions and categorized them into two types: "hot" fibrotic lesions with high levels of surrounding immune cells expressing CD45 and "cold" fibrotic lesions with lower amounts of surrounding immune cells (Figure 1A). These regions of interest (ROIs) were then subjected to digital spatial profiling analysis for gene expression profiling. To minimize the effect of genetic variability, we compared lesions within the same patients. To ensure equivalent amounts of fibroblasts in each ROI, we selected regions with minimal immune cell infiltration and assessed the levels of fibroblast markers before comparing hot and cold lesions (Figure 1B). On obtaining a set of differentially expressed genes, we clustered the data utilizing gene signatures of various stages of pulmonary fibrosis (5) and revealed that hot lesions displayed an early-stage gene signature, whereas cold lesions demonstrated a progressive/end-stage signature (Figures 1C and 1D). Gene set enrichment analysis also identified differentially upregulated pathways between hot and cold lesions (Figure 1E). Hot lesions showed an increase in proproliferative and immune-associated pathways such as KRAS, PI3K/AKT, Myc, mTOR, IL-2, IL-6, IFN, TNF-α/NF-κB (6, 7), linked to proliferation, apoptosis resistance, and immune activation. This suggests that the immune cells may be continually activated in these lesions and, in tandem with the pro-proliferative pathways, contribute to rapidly expanding lesions. In contrast, cold lesions demonstrated the upregulation of typical profibrotic pathways, including epithelial-mesenchymal transition, hypoxia, Wnt, Hedgehog, and TGF-β (6). Figure 1F further shows an enrichment of proproliferative genes in hot lesions and a surge in profibrotic gene expression in cold lesions.

We next corroborated our findings by means of proteomic analysis utilizing multiple protein panels on the same ROIs used in transcriptomic analysis (Figure 2A). A comparison of protein levels between the two lesion types confirmed our previous findings, with hot lesions displaying a pro-proliferative phenotype associated with receptor tyrosine kinase and immune-mediated signaling (Figure 2B). STRING analysis identified an anti-apoptosis/pro-survival and pro-proliferation network in hot lesions (Figure 2C). We further confirmed the upregulated proliferative capacity in hot lesions by staining consecutive slides of the samples with a proliferative marker, PCNA. Our analysis showed a higher proportion of PCNA-stained cells in hot lesions compared with cold lesions, providing further evidence of their greater proliferative capability (Figure 2D). Using multiplex immunohistochemistry, we identified different immune cell types in hot lesions and noted a predominant T cell presence (Figures 2E and 2F), suggesting that these cells may significantly modulate the observed differential gene expression.

Discussion

In hot lesions with prevalent neighboring CD45+ cells, we identified enriched pathways associated with the recruitment of both innate and adaptive immune cells, indicating active diversification of cell types in these lesions. Our investigation showed that T cells predominated in hot lesions, suggesting a primarily T cell–mediated process. This aligns with prior work that highlights a significant, albeit controversial, role of T cells in fibrosis progression (8). The persistent immune response and prolonged interaction with immune cells may contribute to the transition of normal repair processes toward a fibrotic phenotype (9). Despite our study being limited by a small

*These authors contributed equally to this work.

Supported by grants from the National Institutes of Health (R01 HL146802), the University of California Office of the President Tobacco-Related Disease Research Program (T32IR5347), and the Department of Defense Peer-Reviewed Medical Research Program (W81XWH2110086; #PR202411).

Author Contributions: Conception and design: C.-H.C. Development of methodology: S.-W.H. Acquisition of data: D.C.Y., S.-W.H., J.-M.L., and C.-H.C. Analysis and interpretation of data (e.g., statistical analysis, biostatistics, and computational analysis): D.C.Y., S.-W.H., J.O., and C.-H.C. Writing, review, and/or revision of the manuscript: D.C.Y., S.-W.H., and C.-H.C. Administrative, technical, or material support (i.e., reporting or organizing data and constructing databases): S.-W.H., J.O., and C.-H.C. Study supervision: C.-H.C.

Originally Published in Press as DOI: 10.1164/rccm.202303-0372LE on July 24, 2023

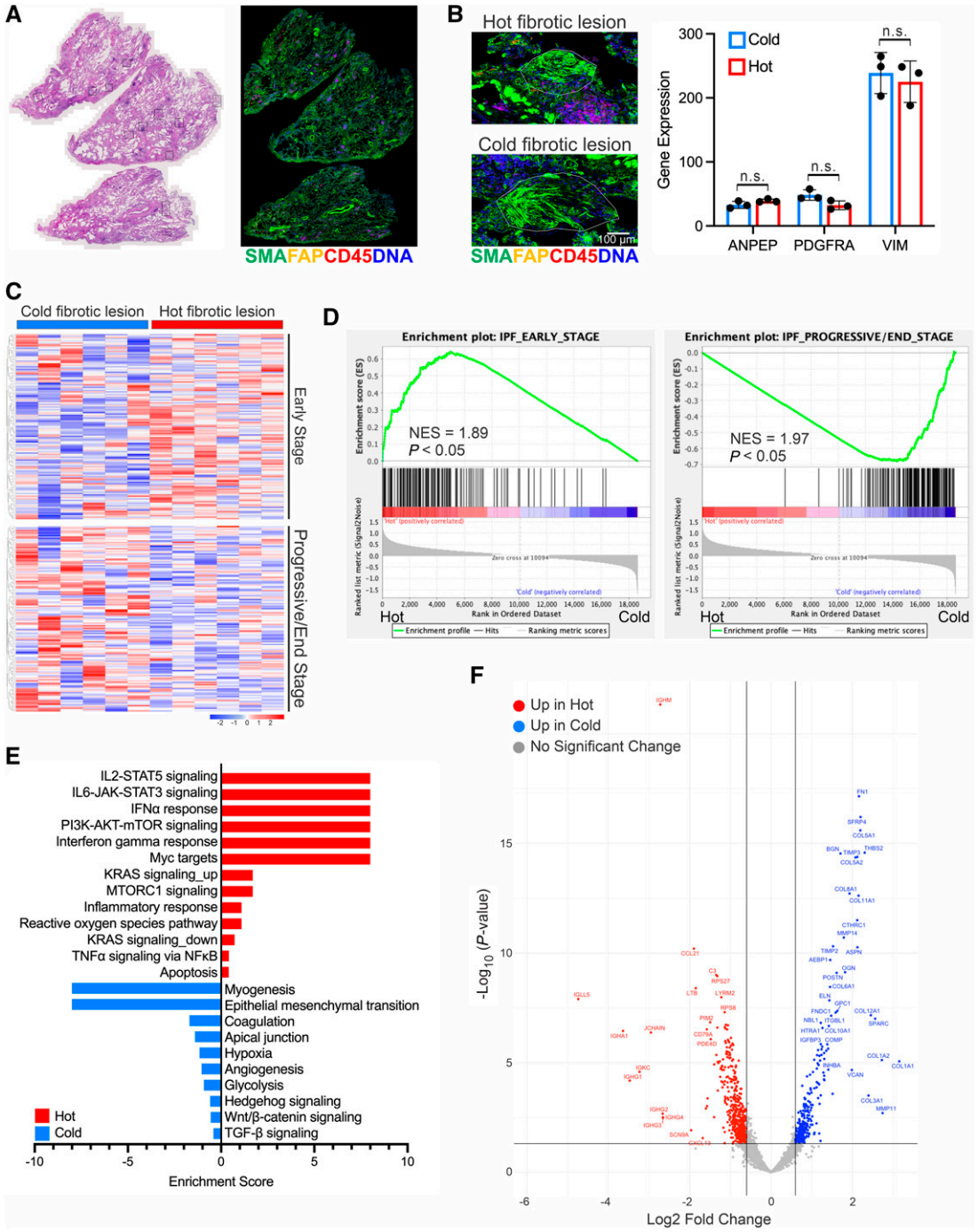

Figure 1. The spatial transcriptomic profile for cold and hot fibrotic lesions of patients with idiopathic pulmonary fibrosis (IPF). (*A*) Representative hematoxylin and eosin– and immunofluorescence-stained sections of lung tissues obtained from six patients who underwent biopsies and histologically confirmed IPF at the University of California–Davis Medical Center. At least two to three biopsy samples from each patient were assessed in the study. The lung sections were stained with antibodies against smooth muscle α-actin (SMA; green) and fibroblast activation protein α (FAP; yellow)—markers for activated fibroblasts—along with the pan-immune cell marker CD45 (red). Nuclear staining was achieved using DAPI (blue). (*B*) Left: representative immunofluorescence-stained images of cold and hot fibrotic lesions from the same patient, taken from a set of three IPF patients. We analyzed a total of 12 regions of interest (ROIs) per patient, ranking them on the basis of the intensity of surrounding CD45+ cells. The three highest intensity ROIs were defined as hot lesions, and the three lowest were defined as cold lesions. We set thresholds for the intensity, which were based on the signal-to-noise ratio (SNR), at >39 SNR for hot lesions and <13 SNR for cold lesions. The circled regions in the images represent the areas selected for RNA sequencing. Right: gene expression of the fibroblast markers ANPEP, PDGFRA, and VIM, in cold and hot fibrotic lesions. Gene expression is expressed as mean ± SD ($n = 3$). Scale bar, 100 μm. (*C*) Heatmaps indicate the enrichments of IPF early and progressive/endstage genes in hot and cold fibrotic lesions, respectively. (*D* and *E*) Gene set enrichment analysis (GSEA) was conducted on the

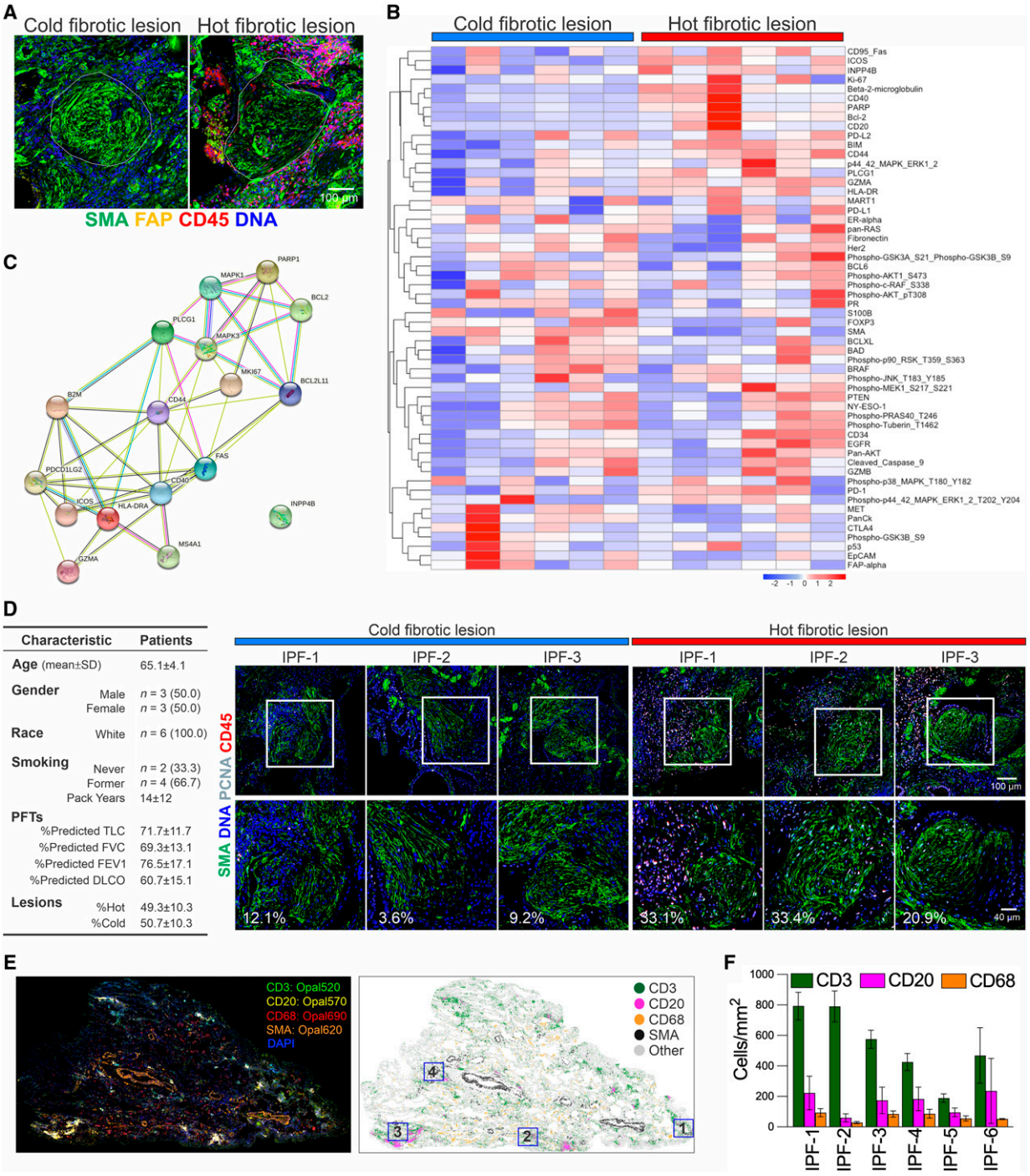

Figure 2. The spatial proteomic profile for "cold" and "hot" fibrotic lesions of patients with idiopathic pulmonary fibrosis (IPF). (*A*) Representative immunofluorescence-stained images for cold and hot fibrotic lesions of three IPF patients with IPF, labeled with antibodies for smooth muscle α-actin (SMA; green), fibroblast activation protein α (FAP; yellow), CD45 (red), and DAPI (blue). As described in Figure 1B, we ranked 12 regions of

Figure 1. (*Continued*). transcriptomes from both cold and hot fibrotic lesions within the same patient. This analysis was performed for a total of three IPF patients. (*D*) Enrichment plots of gene expression signatures for early-stage (left) and progressive/endstage (right) IPF. (*E*) GSEA hallmark analysis results. The two-sided bar chart indicates significant pathway enrichment in hot (red bars) and cold (blue bars) lesions. Enrichment scores are defined as $\log_{10}(1/P \text{ value})$ for hot lesions and $-\log_{10}(1/P \text{ value})$ for cold ones. A false discovery rate (FDR) adjusted *P* value of <0.05 was used to identify significantly enriched pathways. (*F*) The volcano plot displays differentially expressed genes between cold and hot lesions from three IPF patients. Genes with a >1.5-fold change between cold and hot lesions and an FDR of <0.05 are considered significantly differentially expressed. ES = enrichment score; NES = normalized enrichment score; n.s. = no significant difference.

sample size ($n = 6$), we identified an early-stage gene signature and upregulation of pro-proliferation pathways in the hot lesions, suggesting their potential as nascent lesions that are rapidly expanding during the fibrotic process. Conversely, we observed that cold lesions, associated with a late-stage/progressive gene signature, are dominated by typical profibrotic pathways driving transformation and differentiation. This observation clarifies why antifibrotic therapies may have been ineffective in halting fibrotic progression: They primarily target cold lesion features and largely leave the hot lesions, which appear to be actively proliferating, relatively untouched. Although corticosteroids and broad immunosuppressive therapies may dampen proinflammatory features of immune cells near lesions, they may not be sufficient in reducing cell count in the lesions and have limited effects on cold lesions. Therefore, a more effective approach could utilize a combination of antifibrotic and anti-inflammatory agents. Although prior attempts to target immune cells have faced setbacks, promising results have been observed with newer anti-inflammatory agents such as PDE4B inhibitor, which has demonstrated efficacy in slowing fibrosis progression (10).

Our findings present a proof-of-concept for the heterogeneity of fibrotic lesions within the IPF lung. We classified lesions as hot or cold on the basis of the relative presence or absence of CD45+ cells for a more straightforward analysis, given our limited sample size. The inherent heterogeneity of the fibrotic lung suggests that lesions likely exist on a spectrum, rather than fitting strictly into a dichotomous hot or cold phenotype. Further research is needed to explore gene expression gradation associated with the spectrum of immune involvement, temporal changes during disease progression, and precise identification of interacting immune cell types. This could help clarify the prognostic value of these findings and determine critical cell types in fibrosis. These questions could potentially be addressed with an expanded sample set and animal models of progressive fibrosis. ■

Author disclosures are available with the text of this letter at www.atsjournals.org.

Correspondence and requests for reprints should be addressed to Ching-Hsien Chen, Ph.D., Department of Internal Medicine, University of California, Davis, Davis, CA 95616. Email: jchchen@ucdavis.edu.

References

1. Martinez FJ, Collard HR, Pardo A, Raghu G, Richeldi L, Selman M, *et al.* Idiopathic pulmonary fibrosis. *Nat Rev Dis Primers* 2017;3:17074.
2. Nemeth J, Schundner A, Frick M. Insights into development and progression of idiopathic pulmonary fibrosis from single cell RNA studies. *Front Med (Lausanne)* 2020;7:611728.
3. Heukels P, Moor CC, von der Thüsen JH, Wijsenbeek MS, Kool M. Inflammation and immunity in IPF pathogenesis and treatment. *Respir Med* 2019;147:79–91.
4. Eyres M, Bell JA, Davies ER, Fabre A, Alzetani A, Jogai S, *et al.* Spatially resolved deconvolution of the fibrotic niche in lung fibrosis. *Cell Rep* 2022;40:111230.
5. McDonough JE, Ahangari F, Li Q, Jain S, Verleden SE, Herazo-Maya J, *et al.* Transcriptional regulatory model of fibrosis progression in the human lung. *JCI Insight* 2019;4:e131597.
6. Moss BJ, Ryter SW, Rosas IO. Pathogenic mechanisms underlying idiopathic pulmonary fibrosis. *Annu Rev Pathol* 2022;17:515–546.
7. She YX, Yu QY, Tang XX. Role of interleukins in the pathogenesis of pulmonary fibrosis. *Cell Death Discov* 2021;7:52.
8. Deng L, Huang T, Zhang L. T cells in idiopathic pulmonary fibrosis: crucial but controversial. *Cell Death Discov* 2023;9:62.
9. Adler M, Mayo A, Zhou X, Franklin RA, Meizlish ML, Medzhitov R, *et al.* Principles of cell circuits for tissue repair and fibrosis. *iScience* 2020;23:100841.
10. Richeldi L, Azuma A, Cottin V, Hesslinger C, Stowasser S, Valenzuela C, *et al.*; 1305-0013 Trial Investigators. Trial of a preferential phosphodiesterase 4B inhibitor for idiopathic pulmonary fibrosis. *N Engl J Med* 2022;386:2178–2187.

Figure 2. (*Continued*). interest (ROIs) per patient on the basis of the intensity of surrounding CD45+ cells. Sequential slides were utilized for the proteomic and RNA analyses (refer to Figure 1), ensuring that the selected regions for both analyses were the same. The circled regions were selected for proteomic analysis. Scale bar, 100 μm. (*B*) Heatmaps depict the proteomic profiles of cold and hot fibrotic lesions. (*C*) STRING analysis reveals that the proteins enriched in hot fibrotic lesions are involved in anti-apoptotic/pro-survival and pro-proliferation pathways. (*D*) Left: clinicopathologic characteristics of six IPF patients used in the study. Right: the upper panel displays representative immunofluorescence-stained images for cold and hot lesions within the same patients. The hot fibrotic lesions in IPF patients demonstrate increased expression of the proliferation marker PCNA, compared with the cold fibrotic lesions. Immunofluorescence staining was conducted using antibodies against SMA (green), PCNA (gray), and CD45 (red), with DAPI (blue) used for nuclear staining. The lower panel displays higher magnification images of the boxed areas in the upper panel. The percentages displayed on the images represent the proportion of PCNA-positive cells within the lesions. Scale bars: top, 100 μm; and 40 μm (bottom). (*E* and *F*) We performed multiplex immunohistochemistry (mIHC) analysis of immune cell populations surrounding hot fibrotic lesions in six IPF lung tissues. The analysis used an activated fibroblast cell marker, SMA; and immune cell markers, including CD3 for T cells, CD20 for B cells, and CD68 for macrophages. DAPI was used for nuclear staining. (*E*) Left: a representative spectrally unmixed composite mIHC image captured through the Vectra imaging system. Right: a representative phenotype map was created after image analysis using inForm software. Cells were phenotyped on the basis of marker labeling. The boxed areas indicate regions selected for further quantification analysis on the basis of hematoxylin and eosin staining and SMA expression. We analyzed at least three regions per patient. (*F*) Quantification of the density of each cell population in the selected regions, as described in Figure 2E (right), from six IPF patients. Cell counts are shown as mean ± SD (units of measurement are cells per square millimeter). PFTs = pulmonary function tests.